

# 1 **Future Changes in Snowpack, Snowmelt, and Runoff Potential Extremes over** 2 **North America**

3  
4 Eunsang Cho<sup>1,2\*</sup>, Rachel R. McCrary<sup>3</sup>, Jennifer M. Jacobs<sup>4,5</sup>  
5

6 <sup>1</sup>Hydrological Sciences Laboratory, NASA Goddard Space Flight Center, Greenbelt, MD, USA

7 <sup>2</sup>Earth System Science Interdisciplinary Center, University of Maryland, College Park, MD,  
8 USA

9 <sup>3</sup>National Center for Atmospheric Research, Boulder, CO, USA

10 <sup>4</sup>Department of Civil and Environmental Engineering, University of New Hampshire, Durham,  
11 NH, USA

12 <sup>5</sup>Earth Systems Research Center, Institute for the Study of Earth, Oceans, and Space, University  
13 of New Hampshire, Durham, NH, USA  
14  
15

16 \*Corresponding author: Eunsang Cho ([eunsang.cho@nasa.gov](mailto:eunsang.cho@nasa.gov))  
17  
18  
19  
20

## 21 **Highlights**

- 22 • Extreme SWE, snowmelt, and runoff potential maps were developed using a regional  
23 climate model ensemble for historical and future periods
  - 24 • The magnitudes of projected extreme SWE and snowmelt decrease over the CONUS and  
25 southern Canada but increase in Alaska and northern Canada
  - 26 • There is a projected decrease in snowmelt but an increase in runoff potential (e.g. rain-  
27 on-snow) in California and the Pacific Northwest
- 28  
29  
30  
31  
32

33  
34 1<sup>st</sup> Revision submitted to *Geophysical Research Letters*

35 September 18, 2021

**36 Abstract**

37           Snowpack and snowmelt-driven extreme events (e.g., floods) have large societal  
38 consequences including infrastructure failures. However, it is not well understood how projected  
39 changes in the snow-related extremes differ across North America. Using dynamically  
40 downscaled regional climate model (RCM) simulations, we found that the magnitudes of  
41 extreme snow water equivalent, snowmelt, and runoff potential (RP; snowmelt plus  
42 precipitation) decrease by 72%, 73%, and 45%, respectively, over the continental U.S. and  
43 southern Canada but increase by up to 8%, 53%, and 41% in Alaska and northern Canada by the  
44 late 21<sup>st</sup> century. In California and the Pacific Northwest, there is a notable increase in extreme  
45 RP by 21% contrary to a decrease in snowmelt by 31% by the late century. These regions could  
46 be vulnerable to larger rain-on-snow floods in a warmer climate. Regions with a large variability  
47 among RCM ensembles are identified, which require further investigation to reduce the regional  
48 uncertainties.

**49 Plain Language Summary**

50           Even though snow-driven extreme events (e.g., snowmelt floods) have large societal  
51 impacts including infrastructure failures, how much future changes in the magnitude of snow-  
52 driven extremes differ across North America is not well understood. Here, we found that the  
53 magnitudes of future extreme snow water equivalent (SWE) and snowmelt decrease over the  
54 continental United States and southern Canada but increase in Alaska and northern Canada by  
55 the late 21<sup>st</sup> century. In California and the Pacific Northwest, there is a notable increase in runoff  
56 potential (snowmelt plus precipitation) contrary to a decrease in snowmelt itself, suggesting that  
57 these regions may be vulnerable to larger rain-on-snow events in a warmer climate. Also, regions  
58 with a large variability among this study's regional climate models are identified. The large  
59 variabilities in extreme SWE and snowmelt in the western mountain regions and northern  
60 Canada as well as runoff potential in the southeastern United States require further investigation  
61 to reduce the regional uncertainties.

**62 Keywords**

63 Extreme events; Snowpack; Snowmelt; Climate change; Regional climate model; NA-CORDEX

## 64        **1 Introduction**

65            Snowpack, the accumulated snow on the ground, is one of the fastest-changing  
66 hydrologic components under a warming climate (Barnett et al., 2005; Musselman et al., 2017).  
67 The melted water from the snowpack provides the dominant source of water for generating river  
68 flow and recharging groundwater in snow-dominant regions (Li et al., 2017). At the same time,  
69 snowmelt-driven extreme events have potentially large societal and economic impacts on local  
70 and regional communities. Extreme snowmelt including rain-on-snow (ROS) events is an  
71 important driver of severe flood events (Berghuijs et al., 2016; Villarini, 2016; Yan et al., 2018;  
72 2019). During the last few decades, snow-related floods have impacted local communities across  
73 the U.S. and Canada (Stadnyk et al., 2016). The Red River of the North Basin's 1997 flood  
74 caused more than \$5 billion of damages in North Dakota, Minnesota, and Canadian communities  
75 (Todhunter, 2001). The Oroville dam spillway incident in California in February 2017 was  
76 exacerbated by early snowmelt with large ROS events (Henn et al., 2020; Vano et al., 2019). In  
77 the northeastern U.S. and eastern Canada, snowmelt-driven floods have frequently occurred with  
78 ice-jamming, resulting in physical and economic damages to riverine communities (Rokaya et  
79 al., 2018; Yarnal et al., 1997).

80            Civil and water resources engineers rely on historical data sets when making estimates of  
81 design floods to determine the size of infrastructure (e.g. dams and bridges). The current U.S.  
82 government standard design maps such as the National Oceanic and Atmospheric  
83 Administration's National Weather Service Precipitation-Frequency Atlas 14 (NOAA Atlas 14)  
84 are based solely on liquid precipitation data with very limited guidance on snowmelt events  
85 (Fassnacht & Records, 2015; Harpold & Kohler, 2017; Yan et al., 2019). Recently, Cho and  
86 Jacobs (2020) developed 25- and 100-year return level (also known as a recurrence interval that  
87 is an estimated average time between the events to occur) snow water equivalent (SWE) and  
88 snowmelt maps using reliable long-term gridded SWE products and compared these to the  
89 NOAA Atlas 14 standard design maps over the continental U.S. They found that their snowmelt  
90 design values exceeded the standard rainfall design values in 23% of the area in the 44 U.S.  
91 states where the standard maps are available. They emphasized that in most snow-dominant  
92 regions, extreme runoff potential (RP; snowmelt plus precipitation; e.g., ROS), is larger than the  
93 snowmelt itself, indicating that rainfall (or mixed-phase precipitation) during snowmelt is a

94 major contributor to larger snow-driven extreme events. Considering a warmer climate in the  
95 future, more precipitation will likely occur as rainfall instead of snowfall, subsequently resulting  
96 in more intense, large ROS events relative to current conditions (Musselman et al., 2018). Thus,  
97 guidance is needed to design North American infrastructure to accommodate future snow-driven  
98 extreme events (Diffenbaugh et al., 2013; Diffenbaugh, 2017).

99         Projected extreme precipitation is expected to increase by around 20% by the end of the  
100 21st century across the United States under a higher greenhouse gas emission scenario (the  
101 Representative Concentration Pathway [RCP] 8.5) (Easterling et al., 2017). In the winter and  
102 spring seasons, the north-central and northeastern United States and Alaska are projected to  
103 receive more seasonal precipitation by up to 30% relative to the 1976–2005 average (Easterling  
104 et al., 2017). In Canada, winter precipitation (December to February) is also projected to increase  
105 by around 24% over the 21st century, with larger percentage changes in northern Canada (30%;  
106 Bush and Lemmen, 2019). As temperature is expected to increase, a warmer climate forces more  
107 precipitation to fall as rain than snow resulting in a decrease in snowpack with larger and more  
108 frequent rainfall events occurring on shallower snowpacks during winter (Diffenbaugh et al.,  
109 2013). In the Pacific Northwest, for example, snowpack is predicted to decrease by 70% by 2100  
110 under the RCP 8.5 scenario, even though annual precipitation may increase by 10% (Ikeda et al.,  
111 2021). Previous studies predicted declines in snowmelt related flooding in the western U.S. and  
112 Canada, due to projected reductions in spring snowpack with warmer temperatures (Hamlet and  
113 Lettenmaier, 2007; Loukas et al., 2002). However, ROS and mixed-phase precipitation on snow  
114 events are becoming more frequent (McCabe et al., 2007) and are expected to continue in the  
115 future, particularly in regions with higher elevations (Li et al., 2019; Musselman et al., 2018;  
116 Yan et al., 2019). Davenport et al. (2020) also found that winter precipitation shifts toward rain,  
117 in response to warming, cause nonlinear increases in flood size across the western U.S.  
118 indicating that ROS events driven by larger and more frequent rainfall can result in increasing  
119 winter or spring floods.

120         Future projections of snow-related variables have been investigated using different  
121 modeling techniques across multiple time and space scales, including global climate models  
122 (GCMs; Brown and Mote, 2009; Mudryk et al, 2020, Krasting et al, 2013), regional climate  
123 models (RCMs; Mahoney et al., 2021; McCrary and Mearns, 2019; Rasmussen et al, 2011), and  
124 statistical downscaling applied to hydrologic land surface models (Christensen and Lettenmaier,

125 2007). Due to computational constraints, trade-offs must be made in most climate modeling  
126 approaches between the size of the simulation domain, model resolution, and the number of  
127 climate models (RCMs or GCMs). The North American Coordinated Regional Climate  
128 Downscaling Experiment (NA-CORDEX; Mearns et al, 2017) ensemble of RCMs provides a  
129 unique opportunity to examine future changes over a large domain (all of North America) at  
130 relatively high resolutions (25 km) compared to GCMs, for historical and future time horizons  
131 from 1950 to 2100. Additionally the relatively large number of RCM simulations in NA-  
132 CORDEX allows for the exploration of uncertainty (e.g. Kim et al., 2021), highlighting locations  
133 where additional studies may be needed to better understand the impacts of future change over  
134 North America.

135 Although many previous studies have been conducted to predict future changes in SWE  
136 and snowmelt in the U.S. and Canada, projected changes in extreme SWE, snowmelt, and RP  
137 across North America remains poorly understood. In this study, we create and compare spatial  
138 maps of three extreme design metrics, SWE, snowmelt, RP (snowmelt plus precipitation), for  
139 the historical, mid, and late 21st centuries, respectively, using NA-CORDEX. The RP is the  
140 actual amount of water available for runoff originating from melting snow and precipitation  
141 (including snowfall, rainfall absorbed by the snowpack, and percolated rain water through the  
142 snowpack) for a given time period (Yan et al., 2018; 2019; Cho and Jacobs, 2020). We aim to  
143 answer the following three research questions: (1) How much will the magnitude of extreme  
144 SWE, snow melt and RP change by the mid and late 21<sup>st</sup> century? (2) Are there similar spatial  
145 patterns among the three extreme design metrics across North America? (3) Which regions have  
146 the largest differences (uncertainty) among RCM models in future conditions?

## 147 **2 Data and Methodology**

### 148 **2.1 Regional Climate Modeling (RCM) Framework**

149 NA-CORDEX aims to add value to our understanding of climate change at regional scales to  
150 serve the climate change impact and adaptation communities (Mearns et al., 2017). In this study,  
151 daily 25 km spatial resolution SWE and precipitation from nine NA-CORDEX simulations,  
152 which follow the RCP 8.5 scenario, are used to examine changes in extreme SWE, snowmelt,  
153 and RP. The nine simulations from three RCMs with seven GCMs are summarized in **Table S1**

154 and **Text S1**. To offer additional information about the reliability of the NA-CORDEX, the 25-  
 155 year return level NA-CORDEX SWE map is compared to the reference map over the continental  
 156 U.S., which was adopted from Cho and Jacobs (2020) (**Figure S1**).

## 157 **2.2 Annual maximum SWE, snowmelt, and runoff potential**

158 The term “extreme” values (or events) used in this study comes from extreme value  
 159 theory that is widely used to estimate the probability of an unusually large event and the  
 160 magnitude of the large event for a certain probability (Castillo, 2012). The 25-year return period  
 161 design SWE and 7-day snowmelt and RP values are computed using the Generalized Extreme  
 162 Value (GEV) frequency analysis approach with the annual maximum series of each variable  
 163 (Hosking et al., 1990). The GEV distribution function with detailed explanations can be found in  
 164 **Text S2**. The gridded, daily time series for each NA-CORDEX simulation ensemble was used to  
 165 obtain the annual maximum SWE, snowmelt and RP values and to calculate the corresponding  
 166 design extreme values for historical (1976-2005), mid (2040-2069), and late (2070-2099)  
 167 periods. Annual maximum SWE values are the one-day maximum value determined for each  
 168 grid cell daily SWE time series from the October 1 to May 31. Annual maximum 7-day  
 169 snowmelt and RP values are also obtained in that period. A 7-day duration is used to calculate  
 170 the extreme design (25-year return level) snowmelt and RP based on general time periods of a  
 171 response of streamflow to precipitation across the U.S. watersheds (Ivancic & Shaw, 2015;  
 172 Davenport et al., 2020) and persistence days (i.e. multiple days to more than a week) of the  
 173 historical snowmelt and ROS flood events (Pomeroy et al., 2015; Todhunter et al., 2001). The  
 174 annual maximum 7-day RP is calculated by including precipitation into the amount of snow  
 175 ablation (e.g. ROS). RP is defined as the actual amount of water available for runoff from the  
 176 melting snow and precipitation (Yan et al., 2018).

177 Annual maximum 7-day snowmelt ( $Melt_{max,7d}$ ) for each grid is defined as

$$178 \quad Melt_{max,7} = \max [SWE_i - SWE_{i+7}] \text{ when } SWE_i - SWE_{i+7} > 0 \quad (1)$$

179 Annual maximum 7-day RP ( $RP_{max,7d}$ ) includes precipitation, defined as

$$180 \quad RP_{max,7} = \max [Prec_{i+1 \text{ to } i+7} - (SWE_i - SWE_{i+7})] \text{ when } SWE_i - SWE_{i+7} > 0 \quad (2)$$

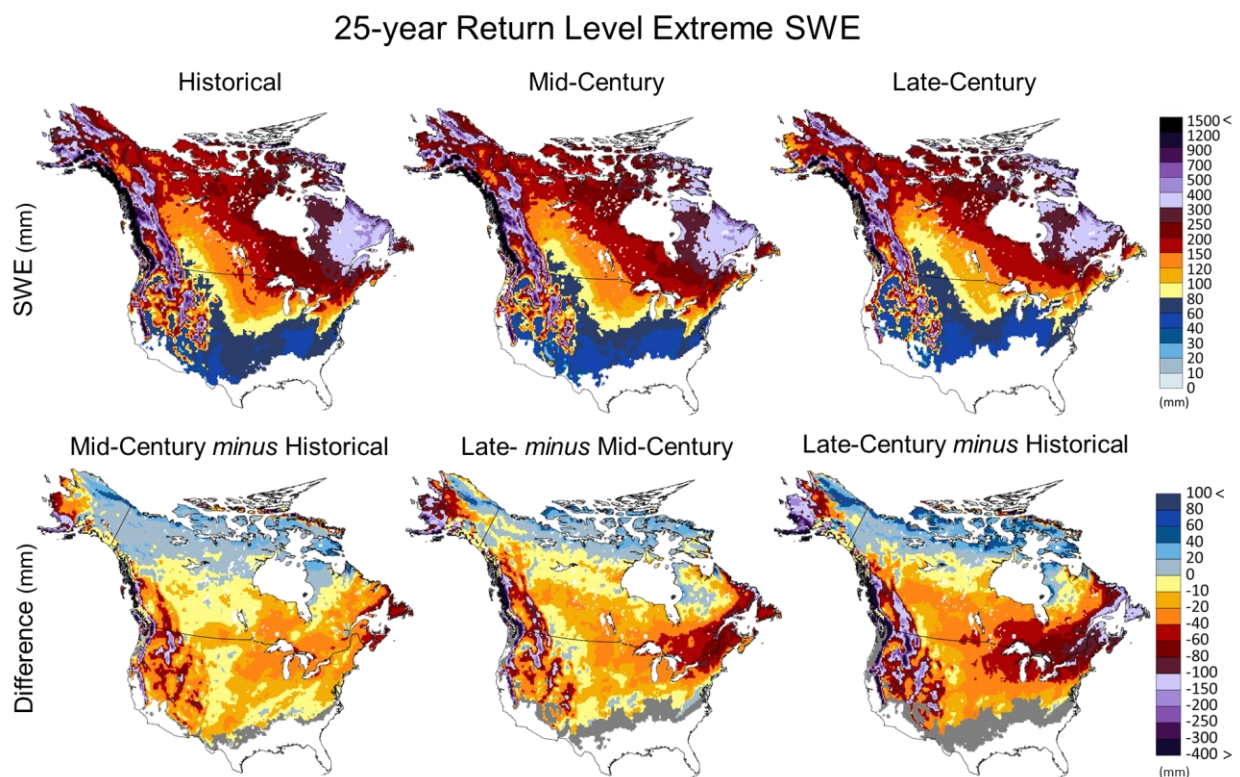
181 where  $i$  is a date from 1 October to 31 May for each year and  $SWE_i$  and  $SWE_{i+7}$  is daily SWE  
 182 (mm) at dates,  $i$  and  $i+7$ , respectively.  $Prec_{i+1\ to\ i+7}$  is accumulated precipitation (mm) between  
 183  $i$  and  $i+7$  dates. To only consider snow-related events, the annual maximum values ( $Melt_{max,7}$  or  
 184  $RP_{max,7}$ ) are selected when positive  $SWE_i - SWE_{i+7}$  (e.g. snow ablation) exists only. As  
 185 compared to changes in SWE itself, the RP is a more relevant variable for quantifying the  
 186 amount of water available to contribute to runoff processes and floods. In previous studies, this  
 187 concept was often referred to using terms such as “water available for runoff” (Yan et al., 2019)  
 188 and “surface water input” (Kormos et al., 2014). The RP calculation used in this study is based  
 189 on the mass balance of snowpack (adopted in Yan et al., 2018), Runoff Potential (output) =  
 190 Precipitation (input) –  $\Delta SWE$  (storage change), indicating that the RP includes water available  
 191 for runoff from the ROS events as well as the mixed-phase precipitation events on snow. While  
 192 magnitude is the major focus of the paper, the timing of annual maximum SWE, snowmelt and  
 193 RP are also a crucial part of the impact from snow changes. The average date of annual  
 194 maximum SWE, snowmelt, and RP averaged over the historical and future periods, as well as  
 195 their future changes are provided in **Figure S2**.

### 196 **3 Results and Discussion**

#### 197 **3.1 Projected changes in extreme SWE**

198 The 25-year return level design SWE maps for the historical (1976-2005), mid (2040-  
 199 2069), and late (2070-2099) century are presented with the difference maps among the three  
 200 periods (**Figure 1**). In the historical period, large extreme SWE values exist in the Cascades in  
 201 the Pacific Northwest, Rocky Mountains, eastern Taiga in Canada (dark purple and black). Low  
 202 SWE values are distributed over the southern United States and Great Plains (blue colors). These  
 203 spatial patterns are retained in future periods, but the magnitude of extreme SWE is projected to  
 204 change. Large reductions in extreme SWE (up to 150 mm and 400 mm for the mid and late 21<sup>st</sup>  
 205 century, respectively) are projected to occur over the western United States and Canada,  
 206 southwest Alaska, and coastal eastern Canada (with the greatest changes in the Pacific Northwest  
 207 and the Rocky Mountains). Extreme SWE is also projected to decrease in the Great Plains, the  
 208 northeastern U.S., Quebec, and Newfoundland and Labrador. The decrease in extreme SWE is  
 209 consistent with previous studies that there are projected reductions in mean SWE or 1 April SWE

210 across the regions (Demaria et al., 2016; Li et al., 2017). Contrary to these regions, SWE  
 211 extremes are projected to increase across high-latitude areas of Canada and northern Alaska. The  
 212 patterns generally correspond to the net winter snowfall projection in Mankin and Diffenbaugh  
 213 (2015). This is likely because warmer temperatures in extremely cold regions will increase  
 214 snowfall by increasing winter precipitation and available moisture (Brown et al., 2017; Cohen et  
 215 al., 2012; Mankin and Diffenbaugh, 2015). An increase in available moisture results in higher  
 216 precipitation efficiency over northern Canada, where the air temperature is still sufficiently cold  
 217 enough to yield snowfall (Ghatak et al., 2010). In most regions, the changes in SWE are more  
 218 notable in the latter part of the century.



219

220 **Figure 1.** 25-year return level design SWE using the annual maximum SWE values for the  
 221 historical (1976-2005), mid (2040-2069), and late (2070-2099) century and their difference  
 222 maps. Gray color along the southern edge in the difference maps indicates regions where the  
 223 SWE no longer exists.

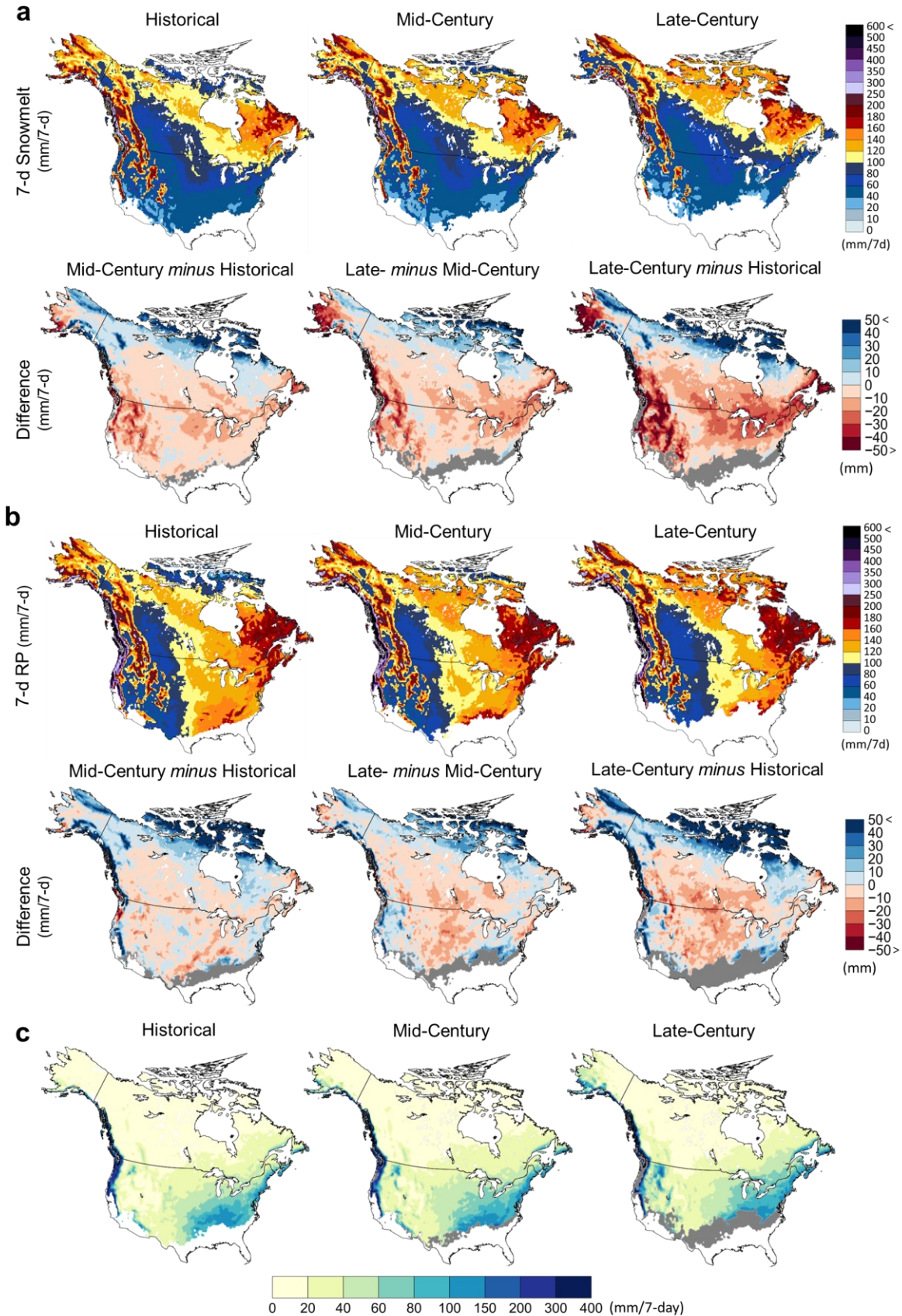
224

225 The magnitude of SWE decline is accompanied by a shift in the timing of peak SWE that  
 226 occurs on average, 12 days earlier than the historical period by mid-century (2040-2069) and 20  
 227 days earlier than the historical period by the late-century (2070-2099) across North America. In  
 228 the Rocky Mountains, the Pacific Northwest, and the southwest Alaska, the timing of the peak

229 SWE is projected to shift earlier by up to 48, 57, and 80 days by the end of the century,  
230 respectively.

### 231 **3.2 Projected changes in extreme snowmelt and runoff potential**

232 The 25-year return level 7-day snowmelt maps have similar spatial patterns to those of  
233 the extreme SWE maps where regions with high SWE have large snowmelt (**Figure 2a**). Large  
234 snowmelt occurs in the Cascades, Rocky Mountains, eastern Taiga in Canada. Projected changes  
235 in the extreme snowmelt between the historical and future periods indicate that decreases will  
236 extend over the continental United States, southern Canada, and Alaska. The greatest changes are  
237 found in the western mountainous regions. In the North Cascades, for example, the magnitude of  
238 extreme 7-day snowmelt is expected to decline by 100 mm/7-day and occur more than 70 days  
239 earlier in the season by the end of the century (**Figure S2**). Similar to the spatial pattern in  
240 extreme SWE, extreme snowmelt is also projected to increase across high-latitude areas of  
241 Canada and Northern Alaska (Brown et al., 2017). The resultant increase of snowmelt in these  
242 regions is nearly equal to the SWE increase. The degree of the projected changes in snowmelt  
243 from historical to mid-century and mid- to late-century also varies by region. In the northern  
244 Canada, much of the increasing snowmelt will occur by mid-century (35%) with modest changes  
245 for the remainder of the century (18% of regional mean values), while the eastern region's  
246 decrease in the melt is greater in the latter portion of the study period (19% relative to 10% in the  
247 earlier portion). In the western U.S., the changes appear to be continuous through the late century  
248 (Mid-century *minus* Historical vs. Late- *minus* Mid-century).



250 **Figure 2.** 25-year return level (a) 7-day snowmelt and (b) RP maps with difference maps for the  
251 historical (1976-2005), mid (2040-2069), and late (2070-2099) century and (c) difference maps  
252 between 7-day RP and snowmelt for each period (gray color along the southern edge in the  
253 difference maps indicates regions where snowmelt (or RP) used to exist, but no longer exists)  
254

255 Despite the projected reduction in extreme SWE and snowmelt, future changes in  
256 extreme RP show that including ROS generally moderates the changes in SWE meltwater  
257 extremes in many regions or even increases RP (**Figure 2b**). Over the Sierra Nevada, Cascade  
258 Range, and the southeast U.S., large increases in RP are projected by the end of the century. In  
259 the Sierra Nevada region, there is a notable increase in extreme RP by 22% (32%) but the timing  
260 of annual maximum RP occurs on average 23 (35) days earlier by the mid (late) century. In the  
261 Cascade Mountain range, the changes in extreme RP are mixed in mid-century (e.g. increases in  
262 southern British Columbia, but decreases in Oregon), but at the end of the century, there are  
263 consistent increases across the entire region. More than a 50 mm/7-day increase in the extreme  
264 RP is projected over northern Canada with RP extremes occurring later in the year.

265 The spatial distributions in the extreme RP, calculated by the annual maximum values of  
266 7-day snowmelt combined with precipitation (e.g. ROS events), are different from those of the  
267 extreme snowmelt (**Figure 2c**). The RP values exceed the snowmelt values by up to 400 mm/7-  
268 day in the Pacific Northwest, California, and the southeast U.S. This indicates that large  
269 precipitation events on snowpacks are the major contributor to extreme RP in these regions. In  
270 the northern Rocky Mountains and southern Alaska, the differences between RP and snowmelt  
271 gradually increase from the historical to mid and late centuries, indicating that the magnitude of  
272 liquid precipitation during the snow meltperiod will increasing. This is attributed in part to  
273 increasing temperatures that will lead to a shift in precipitation partitioning from snow to rain,  
274 particularly for western maritime regions. This has important implications for future spring and  
275 mid-winter floods, which will likely increase in magnitude due to the reduced snow-precipitation  
276 ratios across western North America (Davenport et al., 2020). Flooding from only snowmelt will  
277 decrease in the future, but flooding induced by rain or mixed-phase precipitation in tandem with  
278 melting snowpack will increase in mid-winter and spring. Increases in total winter and spring  
279 precipitation in some regions could additionally contribute to increases in the magnitude of  
280 future spring or mid-winter floods (Bukovsky & Mearns 2020; Mahoney et al, 2021). For  
281 example, in the Pacific Northwest and California, increases in total precipitation are projected in

282 mountain valleys and on the lee-side of the mountains due to an increase in intense atmospheric  
283 river-driven precipitation (Huang et al., 2020). Also, early-season flood risk is expected to  
284 increase in association with increased runoff over heavy-rainy days in California’s Sierra  
285 Nevada (Huang et al., 2018). In the mid-elevations (1500 – 2500 m), the runoff intensity is  
286 projected to increase by 50% and the frequency rises 4 times relative to the historical values  
287 under the RCP 8.5.

288 Even though changes in streamflow are not directly investigated in this study, we can  
289 extrapolate from recent studies that some areas can experience increases in streamflow even with  
290 earlier snowmelt and snowloss (Hammond and Kampf, 2020; McCabe et al., 2018; Robles et al.,  
291 2020). For example, Hammond and Kampf (2020) found that in regions where subsurface water  
292 storage is high and evapotranspiration is low, increases in rainfall and mixed-phase precipitation  
293 during wet winter periods generates higher runoff efficiency (calculated by quickflow, also  
294 known as “direct runoff”, divided by precipitation input) which compensates for the reduced  
295 streamflow that occurs with declining snowpacks. Regarding watersheds where more frequent  
296 winter snowmelt and ROS events are projected to occur and where winter conditions becomes  
297 wetter in the future, larger extreme RP may directly lead to higher runoff efficiency and larger  
298 quickflow, potentially increasing mid-winter flood risk.

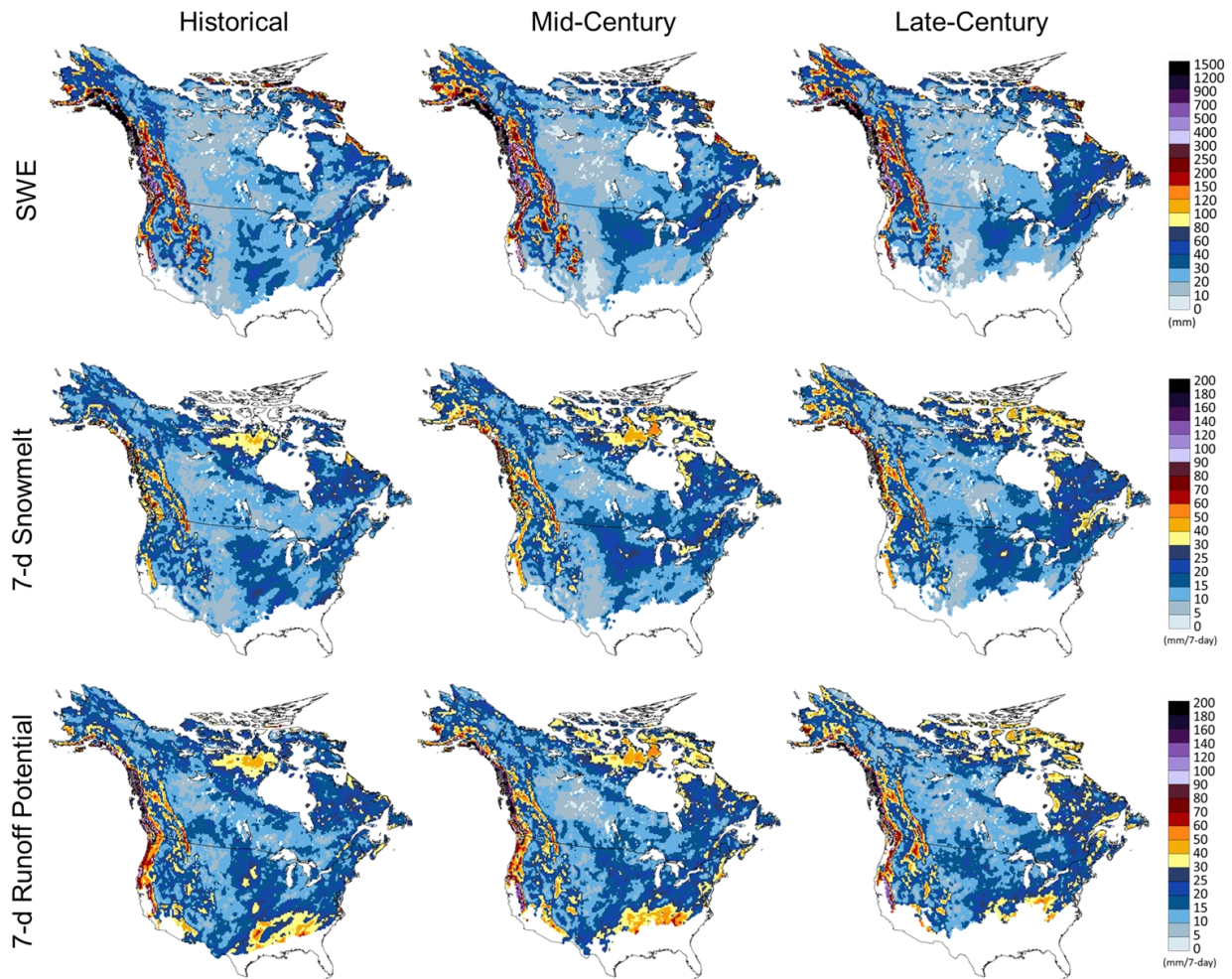
### 299 **3.3 Variations of SWE, snowmelt, and RP among RCMs**

300 To identify regions where there is the largest variability among RCMs, the variability in  
301 the ensemble spread (standard deviation among 9 ensemble members) of extreme SWE,  
302 snowmelt, and RP across North America is examined in **Figure 3**. Coefficient of variation (CV)  
303 maps are also provided in **Figure S3**, which is calculated by dividing the standard deviation by  
304 the ensemble mean. For SWE, the largest uncertainty is in the western mountain regions  
305 including the Pacific Northwest and the Rocky Mountains. This is primarily due to the larger  
306 magnitude of SWE and differences among RCMs to characterize SWE for regions with complex  
307 terrain characteristics. As demonstrated in **Figure S1**, the RCMs generally underestimate  
308 extreme SWE values as compared to a SWE reference dataset in these regions. This is likely  
309 because the 25-km spatial resolution of the RCMs, while much finer than GCM scales, is still too  
310 coarse to represent local heterogenous processes for snow, especially in complex terrains (Ikeda  
311 et al., 2021; Letcher & Minder, 2015; Wrzesien et al., 2017; 2018). RCM SWE output at a finer

312 resolution ( $< 9$  km) compares favorably to reference SWE datasets as compared to the output at  
313 27 km (Wrzesian et al., 2017). Even higher resolution RCM experiments ( $\sim 4$  km) enable to  
314 model microphysical features such as orographical updrafts driving clouds and precipitation (e.g.  
315 Rasmussen et al, 2014; Ikeda et al., 2021). For the CV maps of SWE, there is a relatively large  
316 variation in the central and southern parts of the U.S. (**Figure S3**). While the large uncertainty in  
317 these regions would be less important in terms of extreme events, it can limit the predictability of  
318 agricultural and ecological processes related to snowmelt (Petersky et al., 2018).

319 For snowmelt, there are large variabilities in both the western mountain regions and  
320 northern Canada. With limited SWE variations in northern Canada, the larger variability in  
321 snowmelt is likely due to the temperature differences among the RCMs. Because a large increase  
322 in precipitation (up to 46%) in northern Canada is expected in the late 21<sup>st</sup> century (Bush &  
323 Flato, 2019), this region could be more vulnerable to snow-driven floods than other regions. The  
324 RP maps show larger uncertainties in the southern parts of the United States, which are up to 70  
325 mm/7-day for historical and mid-century. In the late 21st century, SWE no longer exists in the  
326 regions. Because ephemeral snowpack changes in these regions are important for hydrologic and  
327 ecosystem processes (Cho and Jacobs, 2020; Friggens et al., 2018), further study to better  
328 understand the source of these uncertainties is warranted. There are also large RP variations  
329 among RCMs in the Pacific Northwest and California where large shifts in precipitation  
330 partitioning from snowfall to rain as well as increases in extreme atmospheric river-induced  
331 precipitation are expected (Huang et al., 2020). Further investigation is needed to better  
332 understand and harness the RP ensemble spread and in those regions.

Standard deviation of the 25-year 9 RCM models



333

334 **Figure 3.** Standard deviations of the 25-year return level SWE, 7-day snowmelt, and RP maps  
 335 using the nine simulation outputs in the NA-CORDEX ensemble  
 336  
 337

338 **3.4 Regional change in extreme snow-driven events**

339 For design purposes, the granularity of the previous maps is not well suited for decision-  
 340 makers seeking to change policies and engineering practice. Thus, the projected regional changes  
 341 in the extreme SWE and 7-day snowmelt and RP results are summarized in **Figure 4**. Here, total  
 342 volume change maps are provided for 14 regions based on the U.S. National Climate Assessment  
 343 and Canada’s Changing Climate Report boundaries. Projections show regional differences in  
 344 changes to design SWE, snowmelt, and RP. Large decreases in extreme SWE are projected to  
 345 occur over much of North America, except for Alaska and northern Canada (e.g. Yukon,

346 Northwest Territories, and Nunavut). In the continental U.S., projected extreme SWE decreases  
347 by 12 to 37% and 25 to 72% by mid and late 21<sup>st</sup> century, respectively. There is a relatively  
348 small decrease in southern Canada, ranging from 3 to 13% (mid-century) and 11 to 30% (late  
349 century). The widespread SWE decreases across the continental U.S. and southern Canada are  
350 mainly attributable to increasing temperatures that will shift the proportion of total precipitation  
351 that currently falls as snowfall toward rain (Sospedra-Alfonso and Merryfield, 2017). Projected  
352 increases in the extreme SWE in Alaska and northern Canada are due to larger increases in  
353 winter snowfall despite winter temperatures warming by up to 4 °C (Mankin and Diffenbaugh,  
354 2015) because the winter temperature would be still sufficiently cold to generate snowfall  
355 (Ghatak et al., 2010).

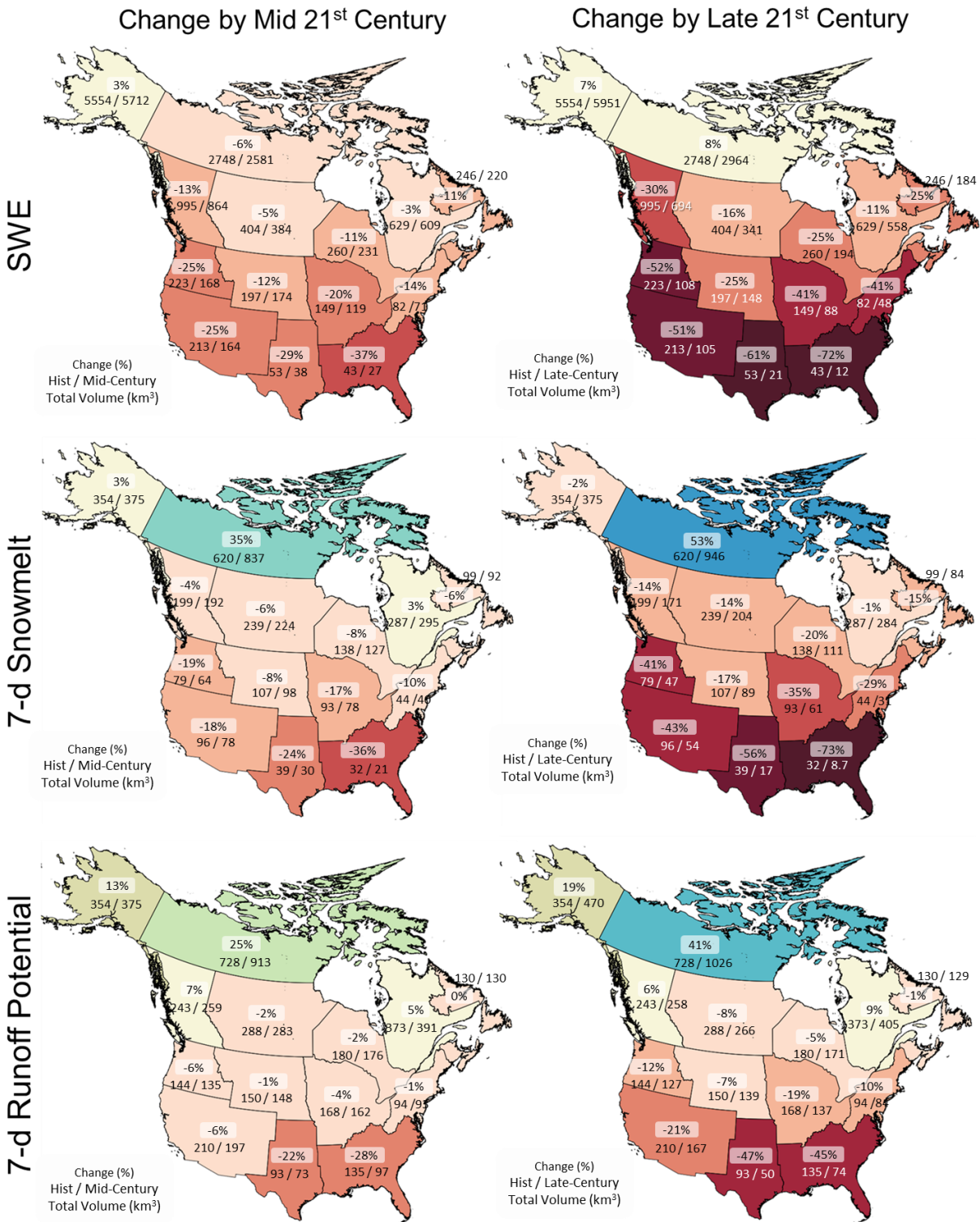
356 Regional changes in the future extreme snowmelt generally have similar spatial patterns  
357 to those of the maximum SWE. However, there is a notable difference in projected snowmelt  
358 between northern and southern Canada. Even though there are minimal increases in extreme  
359 SWE in the high-latitude areas of Canada (Brown et al., 2017; Mudryk et al., 2018), extreme  
360 snowmelt is projected to increase significantly by 35% and 53% by the mid and late 21<sup>st</sup> century,  
361 respectively. Here, warmer temperatures and reduced snowpacks combine to affect the  
362 magnitude of snowmelt-related events, which was noted as an uncertain issue in the recent  
363 Canada's Changing Climate Report (Bush and Lemmen, 2019). In the continental U.S. and  
364 southern Canada, the smaller SWE, rather than warmer temperature, is the more important  
365 control that causes smaller snowmelt events, while in northern Canada the warmer temperatures  
366 drive the larger increases in snowmelt for regions with similar or slightly larger SWE.

367 For extreme RP, there are increases in northern Canada (25% and 41%) as well as Alaska  
368 (13 and 19% by mid and late centuries, respectively). Projected RP changes are consistent but  
369 smaller than projected snowmelt reductions in the continental U.S. Contrary to the decrease in  
370 snowmelt, there is a projected increase in extreme RP in British Columbia (7 and 6% by mid and  
371 late centuries, respectively) even though extreme SWE decreases. Similar increases also occur in  
372 the Pacific Coast Ranges of western North America (in **Figure 2**). Considering that winter  
373 precipitation in the regions is projected to increase by up to 20% from the U.S. National Climate  
374 Assessment (Easterling et al., 2017), the RP increase is likely caused by two reasons: an increase  
375 in winter precipitation itself and a large portion of snowfall being replaced by rain in response to  
376 climate warming (Mankin and Diffenbaugh, 2015). The relative contributions of the drivers may

377 differ by region with elevation ranges because of the elevation-dependent warming and resultant  
378 precipitation phases (Ding et al., 2014; Pepin et al., 2015).

379

## Reginal Change in Extreme Total Volume (25-year Return Level)



381 **Figure 4.** Projected changes in extreme SWE, 7-day snowmelt, and RP over North America  
382 using the U.S. National Climate Assessment and Canada's Changing Climate Report boundaries  
383

#### 384 **4 Conclusion and Future Perspectives**

385 While it is well known that a warmer climate will cause widespread decreases in  
386 snowpack and snowmelt across North America, previous studies have not translated these  
387 projected changes to extreme values appropriate for water resources management and  
388 engineering design. In this study, 25-year return level design SWE and 7-day snowmelt and RP  
389 were estimated for the historic, mid, and late 21st century using a nine-member RCM ensemble  
390 from NA-CORDEX. We found that the magnitude of extreme SWE decreases range from 3 to  
391 37% and 11 to 72% across the continental U.S. and southern Canada by mid and late 21<sup>st</sup>  
392 century, respectively, except for a small increase of about 8% in Alaska and northern Canada.  
393 Generally, the magnitude of extreme snowmelt is informed by the amount of SWE that is present  
394 before melting events occur. However, in the high-latitude areas of Canada extreme snowmelt is  
395 projected to markedly increase by 35% and 53% by the mid and late century, even though there  
396 will be marginal increases in extreme SWE. In California and the Pacific Northwest regions,  
397 there is a notable increase in extreme RP by 21% contrary to a decrease in snowmelt itself by -  
398 31% by the end of the 21<sup>st</sup> century. This is probably attributable to an increasing temperature that  
399 will lead to a shift in the proportion of precipitation partitioning toward rainfall, suggesting that  
400 these regions may be vulnerable to ROS events in a changing climate. Based on the ensemble  
401 spread among the nine RCM models, we found the western mountain regions have the greatest  
402 uncertainties among the models for extreme SWE. For snowmelt, large variabilities were found  
403 in both the western mountain regions and northern Canada. With small SWE variations in  
404 northern Canada, the variability in snowmelt is likely due to the temperature differences among  
405 the RCMs. For extreme RP, there are also large uncertainties in the southeastern U.S., requiring  
406 further investigation to identify potential sources of these regional differences in the RCM's  
407 ephemeral snow estimates.

408 One limitation for this study is the use of relatively coarse spatial resolution (25 km)  
409 climate simulations, for the study of changes in snow in complex terrain. The need for reliable,  
410 high resolution climate modeling to capture local climate processes for snow in complex terrains  
411 (e.g. mountains) has been mentioned before. Considering the inevitable trade-offs among the

412 size of the simulation domain, model resolution, and the number of climate models, mostly due  
413 to limited computational resources, the 25 km spatial resolution of the NA-CORDEX ensemble  
414 simulations is still fine enough to project regional snowpack changes with an ensemble that is  
415 large enough to explore some uncertainty across North America. The large coverage of the NA-  
416 CORDEX simulations allows us to compare how changes vary across the domain and to identify  
417 where additional studies may be needed to better understand the impacts of future change. The  
418 results from this study are expected to provide useful information regarding the magnitude of  
419 future snow-driven extremes under a changing climate as needed to plan, design, and manage  
420 potentially vulnerable water resources and infrastructure.

#### 421 **Data Availability Statement**

422 The NA-CORDEX data used in this study are publicly available at the Climate Data  
423 Gateway at National Center for Atmospheric Research  
424 (<https://www.earthsystemgrid.org/search/cordexsearch.html>). The 25-year return level SWE,  
425 snowmelt, and RP maps and their standard deviation and coefficient of variation maps developed  
426 in this study are available in Hydroshare and can be accessed at  
427 <https://www.hydroshare.org/resource/8efb0f7e743f4a11a4da8b045a37165b>.

#### 428 **Acknowledgments**

429 The authors gratefully acknowledge support from NASA Water Resources Applied  
430 Sciences Program (NNX15AC47G) and the U.S. Department of Energy, Office of Science,  
431 Office of Biological and Environmental Research program under Award Number DE-  
432 SC0016605 and DE-SC0016438. We acknowledge the World Climate Research Programme's  
433 Working Group on Regional Climate, and the Working Group on Coupled Modelling, former  
434 coordinating body of CORDEX and responsible panel for CMIP5. We also thank the climate  
435 modeling groups for producing and making available their model output. We acknowledge the  
436 U.S. Department of Defense Environmental Security Technology Certification Program  
437 (ESTCP) for its support of the NA-CORDEX data archive.

438 **References**

- 439 Adams, R. M., Houston, L. L., & Weiher, R. F. (2004). The Value of Snow and Snow  
 440 Information Services. Report prepared for NOAA's Office of Program, Planning and  
 441 Integration under contract DG1330-03-SE-1097.
- 442 Berghuijs, W. R., Woods, R. A., Hutton, C. J., & Sivapalan, M. (2016). Dominant flood  
 443 generating mechanisms across the United States. *Geophysical Research Letters*, 43(9),  
 444 4382-4390. <https://doi.org/10.1002/2016GL068070>
- 445 Brown, R., Schuler, D., Bulygina, O., Derksen, C., Luoju, K., Mudryk, L., Wang, L. and Yang,  
 446 D. (2017): Arctic terrestrial snow; in Snow Water Ice and Permafrost in the Arctic  
 447 (SWIPA) 2017 Assessment, Arctic Monitoring and Assessment Programme, Oslo,  
 448 Norway, p. 40.
- 449 Bush, E., & Lemmen, D. S. (2019). Canada's changing climate report. Government of Canada=  
 450 Gouvernement du Canada.
- 451 Bukovsky, M.S., & Mearns, L.O. (2020). Regional climate change projections from NA-  
 452 CORDEX and their relation to climate sensitivity. *Climatic Change*, 162(2), 645-  
 453 665. <https://doi.org/10.1007/s10584-020-02835-x>
- 454 Castillo, E. (2012). Extreme value theory in engineering. *Elsevier*.
- 455 Cho, E., & Jacobs, J. M. (2020). Extreme value snow water equivalent and snowmelt for  
 456 infrastructure design over the contiguous United States. *Water Resources Research*, 56,  
 457 e2020WR028126. <https://doi.org/10.1029/2020WR028126>
- 458 Cohen, J. L., Furtado, J. C., Barlow, M. A., Alexeev, V. A., & Cherry, J. E. (2012). Arctic  
 459 warming, increasing snow cover and widespread boreal winter cooling. *Environmental*  
 460 *Research Letters*, 7(1), 014007.
- 461 Davenport, F. V., Herrera-Estrada, J. E., Burke, M., & Diffenbaugh, N. S. (2020). Flood Size  
 462 Increases Nonlinearly Across the Western United States in Response to Lower Snow-  
 463 Precipitation Ratios. *Water Resources Research*, 56(1), e2019WR025571.
- 464 Demaria, E. M., Roundy, J. K., Wi, S., & Palmer, R. N. (2016). The effects of climate change on  
 465 seasonal snowpack and the hydrology of the northeastern and upper Midwest United  
 466 States. *Journal of Climate*, 29(18), 6527-6541.
- 467 Ding, B., Yang, K., Qin, J., Wang, L., Chen, Y., & He, X. (2014). The dependence of  
 468 precipitation types on surface elevation and meteorological conditions and its  
 469 parameterization. *Journal of Hydrology*, 513, 154-163.
- 470 Diffenbaugh, N. S., Scherer, M., & Ashfaq, M. (2013). Response of snow-dependent hydrologic  
 471 extremes to continued global warming. *Nature climate change*, 3(4), 379-384.
- 472 Diffenbaugh, N. S., "What California's dam crisis says about the changing climate," *The New*  
 473 *York Times*, <https://www.nytimes.com/2017/02/14/opinion/what-californias-dam-crisis-says-about-the-changing-climate.html>, accessed on 14 February 2017
- 475 Easterling, D.R., Kunkel, K.E., Arnold, J.R., Knutson, T., LeGrande, A.N., Leung, L.R., Vose,  
 476 R.S., Waliser, D.E., and Wehner, M.F. (2017). Precipitation change in the United States.  
 477 In: *Climate Science Special Report: Fourth National Climate Assessment*, Volume I  
 478 [Wuebbles, D.J., D.W. Fahey, K.A. Hibbard, D.J. Dokken, B.C. Stewart, and T.K.  
 479 Maycock (eds.)]. U.S. Global Change Research Program, Washington, DC, USA, pp.  
 480 207-230, doi: 10.7930/J0H993CC.
- 481 Fassnacht, S. R., & Records, R. M. (2015). Large snowmelt versus rainfall events in the  
 482 mountains. *Journal of Geophysical Research: Atmospheres*, 120, 2375–2381.  
 483 <https://doi.org/10.1002/2014JD022753>

- 484 Ghatak, D., Frei, A., Gong, G., Stroeve, J., & Robinson, D. (2010). On the emergence of an  
485 Arctic amplification signal in terrestrial Arctic snow extent. *Journal of Geophysical*  
486 *Research: Atmospheres*, 115(D24).
- 487 Hamlet, A. F., & Lettenmaier, D. P. (2007). Effects of 20th century warming and climate  
488 variability on flood risk in the western US. *Water Resources Research*, 43(6).  
489 <https://doi.org/10.1029/2006WR005099>
- 490 Harpold, A. A., & Kohler, M. (2017). Potential for changing extreme snowmelt and rainfall  
491 events in the mountains of the western United States. *Journal of Geophysical Research:*  
492 *Atmospheres*, 122, 13–219. <https://doi.org/10.1002/2017JD027704>
- 493 Henn, B., Musselman, K. N., Lestak, L., Ralph, F. M., & Molotch, N. P. (2020). Extreme runoff  
494 generation from atmospheric river driven snowmelt during the 2017 Oroville Dam  
495 spillways incident. *Geophysical Research Letters*, 47(14), e2020GL088189.
- 496 Hernández-Díaz, L., Nikiéma, O., Laprise, R., Winger, K., & Dandoy, S. (2019). Effect of  
497 empirical correction of sea-surface temperature biases on the CRCM5-simulated climate  
498 and projected climate changes over North America. *Climate Dynamics*, 53(1), 453-476.  
499 DOI: 10.1007/s00382-018-4596-2
- 500 Hosking, J. R. M. (1990). L-moments: Analysis and estimation of distributions using linear  
501 combinations of order statistics. *Journal of the Royal Statistical Society: Series B*  
502 *(Methodological)*, 52(1), 105-124.
- 503 Huang, X., Swain, D. L., & Hall, A. D. (2020). Future precipitation increase from very high  
504 resolution ensemble downscaling of extreme atmospheric river storms in  
505 California. *Science Advances*, 6(29), eaba1323.
- 506 Kormos, P. R., Marks, D., McNamara, J. P., Marshall, H. P., Winstral, A., & Flores, A. N.  
507 (2014). Snow distribution, melt and surface water inputs to the soil in the mountain rain-  
508 snow transition zone. *Journal of Hydrology*, 519, 190-204.
- 509 Li, D., Wrzesien, M. L., Durand, M., Adam, J., & Lettenmaier, D. P. (2017). How much runoff  
510 originates as snow in the western United States, and how will that change in the  
511 future?. *Geophysical Research Letters*, 44(12), 6163-6172.
- 512 Li, D., Lettenmaier, D. P., Margulis, S. A., & Andreadis, K. (2019). The role of rain-on-snow in  
513 flooding over the conterminous United States. *Water Resources Research*, 55(11), 8492-  
514 8513.
- 515 Loukas, A., Vasiliades, L., & Dalezios, N. R. (2002). Potential climate change impacts on flood  
516 producing mechanisms in southern British Columbia, Canada using the CGCMA1  
517 simulation results. *Journal of Hydrology*, 259(1-4), 163-188.
- 518 Mankin, J. S., & Diffenbaugh, N. S. (2015). Influence of temperature and precipitation  
519 variability on near-term snow trends. *Climate Dynamics*, 45(3), 1099-1116.
- 520 Mahoney, K., J.D. Scott, M. Alexander; R. McCrary; M. Hughes, D. Swales & M. Bukovsky  
521 (2021). Cool season precipitation projections for California and the Western United  
522 States in NA-CORDEX models. *Climate Dynamics*, 56, 3081-3102.
- 523 McCabe, G. J., Clark, M. P., & Hay, L. E. (2007). Rain-on-snow events in the western United  
524 States. *Bulletin of the American Meteorological Society*, 88(3), 319-328.
- 525 McGinnis, S., & Mearns, L. (2021). Building a climate service for North America based on the  
526 NA-CORDEX data archive. *Climate Services*, 22, 100233.
- 527 Mearns, L.O., et al. (2017). *The NA-CORDEX dataset*, version 1.0. NCAR Climate Data  
528 Gateway, Boulder CO, 01-15-2019, <https://doi.org/10.5065/D6SJ1JCH>.

- 529 Mudryk, L. R., Derksen, C., Howell, S., Laliberté, F., Thackeray, C., Sospedra-Alfonso, R., ... &  
530 Brown, R. (2018). Canadian snow and sea ice: historical trends and projections. *The*  
531 *Cryosphere*, 12(4), 1157-1176.
- 532 Musselman, K. N., Clark, M. P., Liu, C., Ikeda, K., & Rasmussen, R. (2017). Slower snowmelt  
533 in a warmer world. *Nature Climate Change*, 7(3), 214-219.
- 534 Musselman, K. N., Lehner, F., Ikeda, K., Clark, M. P., Prein, A. F., Liu, C., Barlage, M., &  
535 Rasmussen, R. (2018). Projected increases and shifts in rain-on-snow flood risk over  
536 western North America. *Nature Climate Change*, 8(9), 808-812.
- 537 Pepin, N., Bradley, R. S., Diaz, H. F., Baraër, M., Caceres, E. B., Forsythe, N., ... & Mountain  
538 Research Initiative EDW Working Group. (2015). Elevation-dependent warming in  
539 mountain regions of the world. *Nature Climate Change*, 5(5), 424.
- 540 Pomeroy, J. W., Stewart, R. E., & Whitfield, P. H. (2016). The 2013 flood event in the South  
541 Saskatchewan and Elk River basins: Causes, assessment and damages. *Canadian Water*  
542 *Resources Journal/Revue Canadienne Des Ressources Hydriques*, 41(1-2), 105-117.
- 543 Rhoades, A. M., Jones, A. D., & Ullrich, P. A. (2018a). Assessing mountains as natural  
544 reservoirs with a multimetric framework. *Earth's Future*, 6, 1221-  
545 1241. <https://doi.org/10.1002/2017EF000789>
- 546 Rhoades, A. M., Jones, A. D., & Ullrich, P. A. (2018b). The changing character of the California  
547 Sierra Nevada as a natural reservoir. *Geophysical Research*  
548 *Letters*, 45, 13,008– 13,019. <https://doi.org/10.1002/2017EF000789>
- 549 Rokaya, P., Budhathoki, S., & Lindenschmidt, K. E. (2018). Trends in the timing and magnitude  
550 of ice-jam floods in Canada. *Scientific reports*, 8(1), 1-9.
- 551 Sospedra-Alfonso, R., & Merryfield, W. J. (2017). Influences of temperature and precipitation  
552 on historical and future snowpack variability over the Northern Hemisphere in the second  
553 generation Canadian Earth System Model. *Journal of Climate*, 30(12), 4633-4656.
- 554 Stadnyk, T., Dow, K., Wazney, L., & Blais, E.-L. (2016). The 2011 flood event in the Red River  
555 Basin: causes, assessment and damages. *Canadian Water Resources Journal*, 41(1-2), 65-  
556 73. <https://doi.org/10.1080/07011784.2015.1009949>
- 557 Stedinger, J. R., Vogel, R. M., & Foufoula-Georgiou, E. (1993). Chapter 18 Frequency Analysis  
558 of Extreme Events. In D. R. Maidment (Ed.), *Handbook of Hydrology* (pp. 1–66). New  
559 York: DR McGraw-Hill.  
560 <https://sites.tufts.edu/richardvogel/files/2019/04/frequencyAnalysis.pdf>
- 561 Todhunter, P. E. (2001). A hydroclimatological analysis of the Red River of the North snowmelt  
562 flood catastrophe of 1997. *JAWRA Journal of the American Water Resources*  
563 *Association*, 37(5), 1263-1278. <https://doi.org/10.1111/j.1752-1688.2001.tb03637.x>
- 564 Vano, J. A., Miller, K., Dettinger, M. D., Cifelli, R., Curtis, D., Dufour, A., ... & Wilson, A. M.  
565 (2019). Hydroclimatic extremes as challenges for the water management community:  
566 Lessons from Oroville Dam and Hurricane Harvey. *Bulletin of the American*  
567 *Meteorological Society*, 100(1), S9-S14.
- 568 Villarini, G. (2016). On the seasonality of flooding across the continental United  
569 States. *Advances in Water Resources*, 87, 80-91.  
570 <https://doi.org/10.1016/j.advwatres.2015.11.009>
- 571 Yan, H., Sun, N., Wigmosta, M., Skaggs, R., Hou, Z., & Leung, R. (2018). Next-generation  
572 intensity-duration-frequency curves for hydrologic design in snow-dominated  
573 environments. *Water Resources Research*, 54(2), 1093-1108.  
574 <https://doi.org/10.1002/2017WR021290>

- 575 Yan, H., Sun, N., Wigmosta, M., Leung, L. R., Hou, Z., Coleman, A., & Skaggs, R. (2019).  
576 Evaluating next-generation intensity-duration-frequency curves for design flood  
577 estimates in the snow-dominated western United States. *Hydrological Processes*.  
578 <https://doi.org/10.1002/hyp.13673>
- 579 Yarnal, B, D.L Johnson, B.J. Frakes, G.I. Bowles, and P. Pascale (1997). The Flood of '96 and  
580 its socioeconomic impacts in the Susquehanna River Basin, *Journal of the American*  
581 *Water Resources Association*, 33(6), 1299-1312.
- 582 Xu, Z., Rhoades, A. M., Johansen, H., Ullrich, P. A., & Collins, W. D. (2018). An  
583 intercomparison of GCM and RCM dynamical downscaling for characterizing the  
584 hydroclimatology of California and Nevada. *Journal of Hydrometeorology*, 19(9), 1485–  
585 1506. <https://doi.org/10.1175/JHM-D-17-0181.1>  
586